

Calculation of CO₂ gas phase diffusion in leaves and its relation to stomatal resistance

J.W. CARY

Agricultural Research Service, US Department of Agriculture, in cooperation with the University of Idaho, College of Agriculture Research and Extension Center, Kimberly, ID 83341, USA

(Received 13 February 1981; in revised form 23 April 1981)

Key words: photosynthesis, plant stress

Abstract. A new theory and experimental method was developed to measure the diffusion resistance to CO₂ in the gas phase of mesophyll leaf tissue. Excised leaves were placed in a chamber and their net evaporation and CO₂ assimilation rates measured at two different ambient pressures. These data were used to calculate CO₂ gas phase diffusion resistances. A variety of field grown leaves were tested and the effects of various experimental errors considered. Increasing the gas phase diffusion resistance decreased transpiration more than it decreased CO₂ assimilation. It was concluded that gas phase diffusion resistance associated with CO₂ assimilation may sometimes be 100 or 200 s·m⁻¹ greater than the resistance implied by transpiration rates. This may be due to longer path lengths for the CO₂ diffusion, constricted in places by the shape and arrangement of mesophyll cells.

Introduction

The combined stomatal and cuticular resistance to water vapor diffusion is routinely measured with commercial instruments in many controlled environment and field studies. However, the degree of internal leaf resistance to CO₂ diffusion in the gas phase is still an open question, though it is generally considered to be small [3, 4]. If water supplying transpiration is evaporated from the same surfaces in the leaf that also absorb the CO₂ for photosynthesis, the stomatal resistance measured for water would be directly proportional to CO₂ transfer resistance in the gas phase. This has been the classical view [5]. On the other hand, water may evaporate primarily from surfaces just inside the stomata while CO₂ is more extensively transported in the gas phase inside the leaf [1, 2]. Rand [3] developed a mathematical analysis that treats steady state diffusion of water vapor and CO₂ in accord with the concept of CO₂ adsorbed by the cells throughout the interior of the leaf, while water evaporates mainly from cell walls near the stomata. Tyree and Yianoulis [5] using computer simulation also present evidence supporting this viewpoint.

Conceivably the gas phase CO₂ diffusion resistance inside leaves could be a significant variable. The anatomy of leaves varies widely among families. The stomatal number and leaf size of a single variety may be affected by previous light, temperature, and soil water conditions. The thickness and

consequently the gas phase geometry in most leaves changes throughout the day as their water potential decreases. All of these phenomena could be involved in plant adaptation to periods of environmental stress through their effects on CO_2 diffusion and assimilation relative to transpiration.

One might consider measuring internal leaf CO_2 diffusion resistance by observing the passage of an inert gas from a chamber on one surface of a leaf into a chamber on the other side. However, the result would not be the 'effective' CO_2 resistance because CO_2 diffusion pathways in the leaf are affected by the absorption of CO_2 into the liquid phase at specific locations. A better alternative may be to measure the CO_2 assimilation at different ambient pressures. Gas diffusion coefficients are inversely proportional to the total pressure. Consequently, the pressure dependence of assimilation provides a way to measure the effect of gas phase diffusion resistance on photosynthesis.

Theory

One may define 'effective' CO_2 transport resistances in the gas phase as

$$F = \frac{C_a - C_w}{r_g} = \frac{C_a - C_w}{r_s + r_{gm}}, \quad (1)$$

where F is the net CO_2 assimilation in $\text{mg CO}_2 \cdot \text{m}^{-2} \cdot \text{s}^{-1}$; C_a is the ambient CO_2 concentration in $\text{mg} \cdot \text{m}^{-3}$; C_w the concentration of CO_2 at the gas-liquid interfaces in the leaf where CO_2 is being absorbed; r_s is the combined boundary layer, stomatal and cuticular resistances to CO_2 diffusion in $\text{s} \cdot \text{m}^{-1}$; r_g is the total resistance to CO_2 diffusion in the gas phase and r_{gm} is CO_2 diffusion resistance in the gas phase of the mesophyll tissue.

The ambient pressure dependence of equation (1) may be expressed as

$$Fr_g = C_a - C_w \quad (2)$$

and

$$F_o \gamma r_g = C_a - C_{wo}, \quad (3)$$

where F_o is the net assimilation of CO_2 at some pressure greater than atmospheric, γ is the absolute pressure at which F_o was measured divided by the atmospheric pressure and C_{wo} is the concentration of CO_2 at the cell walls around the chloroplasts when the pressure is raised above atmospheric with C_a held constant. Increasing the ambient pressure increases the diffusion resistance; consequently, the concentration of CO_2 will decrease adjacent to the cells that are adsorbing CO_2 . This decrease in CO_2 can be estimated as a perturbation of the value of C_w at ambient pressure by using a simple empirical function that converges to the known limits; i.e., $C_w \rightarrow C_a$ as $r_g \rightarrow 0$ and, when photorespiration is small (1% ambient O_2 or a C_4 plant), $C_w \rightarrow 0$ as $r_g \rightarrow \infty$. Let us define ϵ at constant C_a such that

$$C_w = C_a \exp -\epsilon r_g. \quad (4)$$

Then, for a small change in F brought about by a change in r_g , where ϵ is a specific constant for any given leaf under otherwise unchanged conditions, equations (2) and (3) may be rewritten as

$$Fr_g = C_a (1 - \exp - \epsilon r_g) \quad (5a)$$

and as

$$F_o \gamma r_g = C_a (1 - \exp - \epsilon \gamma r_g). \quad (5b)$$

Solving the first of these relations for ϵ and using the result to replace ϵ in the other leads to

$$f(r_g) = \frac{C_a}{\gamma F_o} \left(1 - \left(1 - \frac{Fr_g}{C_a} \right)^\gamma \right) - r_g = 0. \quad (6)$$

Equation (6) is nonlinear with respect to r_g , but r_g can be found using a programmable calculator and the Newton-Raphson iteration formula

$$r_{g(n+1)} = r_{g(n)} - \frac{f(r_g)}{f'(r_g)}, \quad (7)$$

$$\text{where} \quad f'(r_g) = \frac{df(r_g)}{dr_g} = \frac{F}{F_o} \left(1 - \frac{Fr_g}{C_a} \right)^{\gamma-1} - 1. \quad (8)$$

A reasonable guess for the gas phase resistance is entered in equations (6) and (8) for r_g and also for $r_{g(n)}$ in equation (7). Equation (7) then gives a value for $r_{g(n+1)}$ that is used in equations (6), (7), and (8) to find $r_{g(n+2)}$. The process is repeated until further iterations result in little improvement in the estimate of $r_{g(n)}$; for example, $|r_{g(n)} - r_{g(n+1)}| < 0.1$. This value for $r_{g(n+1)}$ is the solution for r_g in equation (6). If too small a value for r_g is initially entered, $r_{g(n)}$ will converge to zero, which is a trivial solution for equation (6). Thus, the first guess should be on the high side, but not so large that the term $(1 - Fr_g/C_a) < 0$. The value of r_g can also be found from (6) using a 'zero of functions' routine that is available in some calculator software packages.

Experimental procedures

Measurements of F , F_o , C_a and r_g were made in the leaf chamber sketched in Figure 1. The area enclosed by the ring was 24.2 cm^2 which was exposed to a mercury light that delivered $700 \mu\text{E} \cdot \text{m}^{-2} \cdot \text{s}^{-1}$ inside the chamber. The rest of the leaf was shaded from direct light to reduce transpiration and temperature rise.

The gas was mixed from cylinders of O_2 , N_2 and $\text{N}_2 + \text{CO}_2$. The mixture was adjusted to any desired composition using two sets of pressure regulators followed by individual micrometer needle valves between each tank

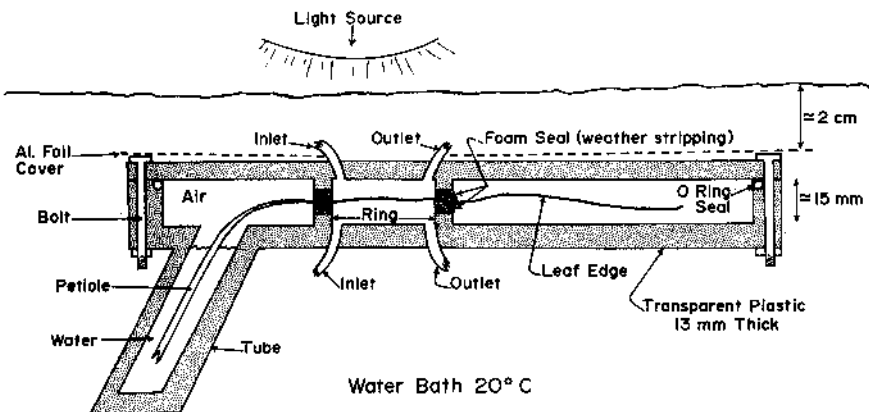


Figure 1. Cross section diagram showing an excised leaf in the pressure chamber submerged in a constant temperature bath, but exposed to a photosynthetically active light source. The dashed line represents an aluminum foil cover to reduce evaporation from the bulk of the leaf.

and the mixing manifold. The mixed gas was passed through a flow meter, infrared CO_2 analyser, and a paramagnetic O_2 analyser.* The needle valves were adjusted to give the desired mixture. The inlet and outlet of the leaf chamber was then connected between the mixing manifold and the flow meter, and the gases allowed to come to steady state with the area of leaf exposed in the ring. Stomatal and boundary layer resistance, r_s , was calculated in the normal way from the leaf temperature (measured with a thermocouple) and the rate of transpiration (measured with a dewpoint, mirror-type instrument connected in series with the gas analysers and flow meter). The boundary layer resistance was measured as $110 \text{ s} \cdot \text{m}^{-1}$ at $1 \text{ l} \cdot \text{min}^{-1}$ flow rate by using a wet filter paper in place of the leaf. The leaf temperature was held at approximately 20°C .

Measurements of F_o at higher than atmospheric pressure was done at the same flow rate and temperature following the same routine for measuring F , except that a needle valve was placed in the gas line just after it left the leaf chamber. The valve was closed enough to bring the pressure in the chamber to the desired level. This left the flow meter and gas analysers at atmospheric pressure so that their calibrations did not change.

The measurements of F_o were made at 60 kPa above atmospheric which gave γ a value of 1.68 corrected for altitude. Pressure was measured with a commercial gauge checked against a Hg column. Values of r_s were also

*Beckman Model 865 CO_2 analyser, Beckman Model C-2 O_2 analyser (calibrations checked with standard gases) floating ball gas flow meters, Cambridge Model 990 dewpoint hygrometer and Wescor digital TH-65 thermocouple reader $\pm 0.1^\circ \text{C}$ (calibrations checked with water adsorbed in a silica gel column from steady state gas streams).

Trade names and company names are included for the benefit of the reader and do not imply any endorsement or preferential treatment of the product listed by the US Department of Agriculture.

measured at the higher pressure, and checked to ensure they were 1.68 times greater than r_s measured at atmospheric pressure before the data were accepted for use in equation (6). Use of (6) also requires that C_a be held constant when the pressure is increased in the leaf chamber. Consequently, the mixing valves were adjusted so the analyser registered a value about 1.68^{-1} times smaller for CO_2 concentration in the gas stream entering the pressurized chamber, as compared to the concentration at normal pressure. The oxygen concentration was similarly adjusted. The flow rate was held constant at 1 l per minute at atmospheric pressure by increasing the amount of nitrogen.

Leaves were taken from field grown plants just prior to placement in the chamber taking care to keep them enclosed in a plastic bag with their petioles submerged in water. About 1 hour was allowed for each leaf to reach steady state after placement in the chamber. Then, 20 to 40 minutes was allowed to achieve steady state following changes in gas concentration or total pressure.

Results and discussion

Measurements of net CO_2 uptake and stomatal resistance at ambient pressure and at 1.68 times ambient pressure are shown for 3 leaves in Table 1. The ambient values of C_a are those measured by the gas analyser which was always at atmospheric pressure. Consequently the real concentration of CO_2 reaching the leaf was 1.68 times greater when the pressure around the leaf was raised to 1.68 times atmospheric. These pressure corrected values are shown in column 7 as a check on how well the gas mixture was controlled. The pressure adjusted stomatal resistance and CO_2 uptake are also shown in separate columns. For stable leaves, examples 2 and 7, the pressure corrected stomatal resistances, $1.68^{-1} r_s$, were near the resistances measured at ambient pressure, as required by the theory. On the other hand, the pressure adjusted assimilation rates, $1.68 F_o$, were always significantly larger than those observed at atmospheric pressure. This shows that increasing the gas phase diffusion resistance decreases the evaporation of water relatively more than it reduces the uptake of CO_2 , a result that is not unexpected [5].

The data in Table 1 may be used to find values for r_g from equation (6). For leaf No. 2, the pressure corrected values of r_s and C_a for observation No. 2 are reasonably close to the values measured during observation No. 3. Consequently, the values $F = 0.23$, $F_o = 0.18$ and $r_s = 300$ were used to find $r_g = 1090$ as shown in Table 2. Likewise observations 2 and 3 for leaf No. 7 give a value of $r_g = 500 \text{ s} \cdot \text{m}^{-1}$. The possible error associated with these two values of r_g are shown in Figure 2. In 2A, the effect on r_g is given by the dashed line for a range of values of F varying around the observed value of 0.23 on leaf No. 2. The solid line gives the same information for

Table 1. Measurements of net CO_2 fixation and stomata plus boundary layer resistance at different levels of CO_2 and ambient pressures. Leaf numbers correspond to the leaves described in Table 2

| Leaf No. | Observation No. | Net fixation $\text{mg CO}_2 \cdot \text{s}^{-1} \cdot \text{m}^{-2}$ | C_a $\text{mg} \cdot \text{m}^{-3}$ | r_s $\text{s} \cdot \text{m}^{-1}$ | Pressure | $1.68 C_a$ | $1.68^{-1} r_s$ | $1.68 F_o$ |
|----------|-----------------|--|--|---|-------------|------------|-----------------|------------|
| 2 | 1 | 0.19 | 404 | 390 | ambient | | | |
| | 2 | 0.18 | 242 | 530 | 1.68 · amb. | 406 | 310 | 0.26 |
| | 3 | 0.23 | 406 | 290 | ambient | | | |
| 7 | 1 | 0.86 | 503 | 390 | 1.68 · amb. | 844 | 230 | 1.45 |
| | 2 | 0.83 | 509 | 340 | 1.68 · amb. | 854 | 200 | 1.40 |
| | 3 | 1.20 | 848 | 200 | ambient | | | |
| 9 | 1 | 0.68 | 521 | 730 | 1.68 · amb. | 874 | 430 | 1.13 |
| | 2 | 0.81 | 515 | 650 | 1.68 · amb. | 864 | 390 | 1.36 |
| | 3 | 0.85 | 858 | 340 | ambient | | | |
| | 4 | 0.67 | 862 | 510 | ambient | | | |
| | 5 | 0.73 | 538 | 760 | 1.68 · amb. | 903 | 450 | 1.19 |

Table 2. Various components of CO_2 leaf diffusion resistances in leaves collected from the field. Columns showing CO_2 , $\% \text{O}_2$, F and r_s give the ambient conditions for which r_g was calculated with equation (6). The symbols are defined by equation (1) and the leaves were from pinto bean (*Phaseolus vulgaris*), sugarbeet (*Beta vulgaris*), corn (*Zea mays*), cucumber (*Cucumis sativas*), grape (*Vitis labrusca*), garden iris (*Iris pseudocorus*), and wild sunflower (*Helianthus annuus*)

| Leaf No. | CO_2 $\text{mg} \cdot \text{m}^{-3}$ | $\% \text{O}_2$ | F | $\text{s} \cdot \text{m}^{-1}$ | | Leaf description |
|----------|--|-----------------|------|--------------------------------|-------|---------------------------------------|
| | | | | r_g | r_s | |
| 1 | 374 | 1 | 0.67 | 430 | 200 | Beet, expanding with large sink |
| 2 | 406 | 1 | 0.23 | 1090 | 300 | Beet, mature, showing N chlorosis |
| 3 | 394 | 1 | 0.36 | 1030 | 400 | Beet, expanded, soil water stressed |
| 4 | 384 | 1 | 0.52 | 250 | 240 | Beet, mature |
| 5 | 612 | 21 | 0.56 | 400 | 260 | Beet, flaccid |
| 6 | 634 | 21 | 0.57 | 340 | 320 | Bean, fully expanded, plant blooming |
| 7 | 848 | 1 | 1.20 | 500 | 200 | Sunflower, expanding, plant blooming |
| 8 | 846 | 1 | 0.41 | 1160 | 670 | Iris, mature |
| 9 | 858 | 1 | 0.85 | 140,330 | 340 | Corn, near top of plant |
| 10 | 622 | 1 | 0.86 | 200 | 240 | Bean, mature, pods filling |
| 11 | 651 | 1 | 0.58 | 560 | 470 | Grape, fully expanded |
| 12* | 396 | 1 | 0.32 | 540 | 460 | Grape, nearly expanded |
| 13* | 398 | 1 | 0.53 | 560 | 300 | Cucumber, fully expanded |
| 14* | 406 | 1 | 0.36 | 1140 | 550 | Bean, mature, filling pods |
| 15* | 406 | 1 | 0.48 | 440 | 370 | Corn, near top of plant, ears filling |
| 16* | 390 | 1 | 0.58 | 330 | 220 | Sunflower, expanded |
| 17* | 390 | 1 | 0.48 | 650 | 340 | Beet, expanded, low N soil |

* Measurements made on the underside of the leaf with the topside closed off from gas flow.

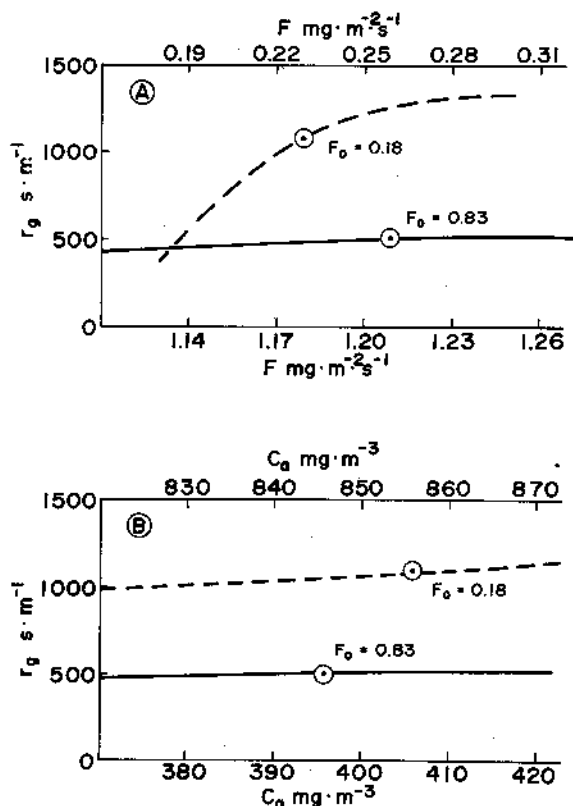


Figure 2. The effect of errors in the measurement of CO₂ fixation rates, F , (part A) and ambient CO₂ concentrations C_a , (part B) on the value of r_g calculated from equation (6) using data from Table 1 for leaves No. 2 (beet, $F_0 = 0.18$) and No. 7 (sunflower, $F_0 = 0.83$). The points show the observed values of F and C_a while the curves through the points show the changes in r_g that would result from different values of F or C_a .

leaf No. 7. Figure 2B shows the effect on r_g of error in the measurement of ambient CO₂ concentration. It is not difficult to measure the steady state uptake of CO₂ with an accuracy of $\pm 0.03 \text{ mg} \cdot \text{m}^{-2} \cdot \text{s}^{-1}$ on a stable leaf. However, this much error in F can cause an uncertainty of several hundred $\text{s} \cdot \text{m}^{-1}$ in calculated values of r_g when the net fixation rate is low (leaf 2). On the other hand the uncertainty becomes less at high CO₂ fixation rates (leaf 7). Possible errors in the measurement of ambient CO₂ have less effect on calculations of r_g as shown in Figure 2B. However not having the same concentration of CO₂ around the leaf at ambient and at γ times ambient pressure could cause a larger error because that would affect the measured difference between F and F_0 .

Data from leaf No. 9 shown in Table 1 are examples of problems that

occur when the leaf is not stable during the course of measurements. Observations 2 and 3 provide the best match of ambient and pressure corrected values of r_s and C_a . While both $1.68r_s$ and $1.68C_a$ are a bit above r_s and C_a at ambient pressure, they are compensating to some degree. Observations 2 and 3 give $r_g = 130$. Differences in F between observations 3 and 4 were evidently due to an increase in stomatal resistance. A linear interpolation of these values give $F = 0.76$ at $r_s = 450$. Using these interpolated numbers with observations 1 and 5 gives $r_g = 140$ and 330 , respectively. Thus while interpolation can be used to calculate values for leaves that are somewhat unsteady, the results will be less certain.

Values for the CO_2 diffusion resistances defined in equation (1) are shown in Table 2 for a variety of leaves. All the resistance values listed in Table 2 are with respect to atmospheric pressure and the conditions of CO_2 , percent O_2 and F specified in columns 2, 3 and 4. The stomatal and boundary layer resistance, r_s , subtracted from the r_g values calculated from equation (6) gives r_{gm} ; i.e., the resistance to CO_2 diffusion in the gas phase of the mesophyll spaces. Experimental uncertainty in the values given for r_{gm} must be recognized, possibly in the neighborhood of $\pm 150 \text{ s} \cdot \text{m}^{-1}$ for stable leaves with intermediate rates of CO_2 absorption. The largest values of r_{gm} in Table 2, leaves 2, 3, 8 and 14 are associated with low rates of CO_2 uptake and so as shown in Figure 1A are subject to experimental uncertainties of several hundred $\text{s} \cdot \text{m}^{-1}$. This may be the reason that these values are so large. There is also a possibility that increasing the ambient pressure reduced their CO_2 uptake by some unknown mechanism other than increased gas phase diffusion resistance. The two negative values of r_{gm} , leaves 9 and 10, also presumably result from experimental error. As already pointed out, the stomatal resistance of leaf 9 was not particularly stable during the measurement period.

Experimental errors may be reduced to some extent through selection of the CO_2 and O_2 concentrations. Results from several combinations are reported in Table 1. The O_2 concentration may be kept low to enhance the response of F to changes of internal CO_2 and, consequently, to r_{gm} . Low O_2 levels also reduce any effects of CO_2 generated by photorespiration as required by the boundary conditions for equation (4), though this is not a large factor as long as the pressure induced change in C_w is moderate. Levels of C_a in the neighborhood of $400 \text{ mg} \cdot \text{m}^{-3}$ give a good response to changes in gas diffusion resistance due to the slope of the photosynthesis response curve to CO_2 concentrations in this range. On the other hand, higher levels of CO_2 increase F which has a favorable effect on reducing error as seen in Figure 1A.

One cannot necessarily expect the value of r_{gm} to be independent of stomatal resistance or ambient CO_2 concentrations. If the stomatal resistance is high, the internal CO_2 concentration will be reduced and the CO_2 may not diffuse very far into the mesophyll tissue before absorption into

the liquid phase. This would decrease r_{gm} . On the other hand, increasing C_a may result in a greater amount of CO_2 diffusing farther into the leaf before entering the liquid phase with a corresponding increase in r_{gm} . The number and distribution of stomata are important in this aspect. Changes in leaf water content may also affect r_{gm} because of the changes that occur in the air filled pore size distribution of the mesophyll tissue as its cells shrink and swell.

The data in Tables 1 and 2 are presented primarily to illustrate the method and to give the reader a feeling for the range of values that may be encountered subject to the experimental uncertainties involved. Nevertheless, it does appear that gas phase resistance to CO_2 uptake may sometimes be 100 or $200 \text{ s} \cdot \text{m}^{-1}$ greater than diffusion resistance inferred by transpiration rates.

References

1. Aston MD and Jones MM (1976) A study of transpiration surfaces of *Avena sterilis* L. var. Algerian leaves using mono silicic acid as a tracer for water movement. *Planta (Berl.)* 130:121–129.
2. Meidner H (1975) Water supply, evaporation, and vapour diffusion in leaves. *J Exp Bot* 26:66–73.
3. Rand RH (1977) Gaseous diffusion in the leaf interior. *Trans ASAE* 20:701–704.
4. Teuhunen JD, Weber JA, Filipek LH and Gates DM (1977) Development of a photosynthesis model with an emphasis on ecological applications. III. Carbon dioxide and oxygen dependencies. *Oecologia (Berl.)* 30:189–207.
5. Tyree MT and Yianoulis P (1980) The site of water evaporation from sub-stomatal cavities, liquid path resistances and hydroactive stomatal closure. *Ann Bot* 46:175–193.